Progress In Electromagnetics Research C, Vol. 126, 39–47, 2022

Compact Wideband Single-Side Printed Antenna for Microwave and Millimeter-Wave Wireless Communications

Hagar A. Farag[1], Asmaa E. Farahat[2], Ahmed I. Bahnas[3], and Khalid F. A. Hussein[4, *]

Abstract—A novel miniature antenna is proposed for wireless communications in the K-band and Ka-band of the electromagnetic spectrum. The frequency band of this antenna extends from 18 to 40 GHz. The proposed antenna is a planar monopole printed on a thin dielectric substrate of 0.25 mm thickness. To enhance the frequency bandwidth of this antenna, it is constructed as five circular sectors placed with sequential rotations and merged to form a multi-leaf shaped monopole patch antenna. To enhance the antenna performance, the monopole patch is fed through a coplanar waveguide (CPW) structure. This enables the overall antenna structure and feeding CPW to be printed on only one side of the dielectric substrate leaving the other side blank, which reduces the dielectric loss and enhances the radiation efficiency. The assessment of the antenna performance is achieved through simulation as well as experimental work. A prototype of the antenna is fabricated for this purpose. The experimental results show excellent agreement with the simulation ones. The antenna is printed on a Rogers' RO3003 substrate of 0.25 mm thickness. It is shown, through both results, that the antenna has 2.2 : 1 ratio bandwidth, 76% percentage bandwidth, and 278 bandwidth-dimension ratio. The radiation efficiency is maintained above 99% over the entire bandwidth (18–40 GHz).

1. INTRODUCTION

During the past few decades, a lot of research works in the field of planar antennas have developed various printed antenna designs for dual band, multi-band, wideband, ultra-wideband operation for different wireless applications [1–6]. The spectra of the L, S, C, and X-bands of the microwave frequency for wireless communications have been crowded with growing number of users and applications, and are going to be rapidly saturated. For this reason, it has recently been convenient to shift the focus of research work and the interest of antenna designers toward the higher frequency bands represented by Ku-, K-, and Ka-bands of the frequency [2]. Over the last decade, antenna designers have been concentrating their research work on investigating the employment of planar and printed antenna structures to operate in the Ku, K-, and K-bands for satellite and radar applications [2]. However, the researchers are still working hard to optimize the planar antenna structures so as to produce high gain and sufficient bandwidth for providing the high data rates required by such applications.

Modern satellite communication systems require high data rate for the uplink, downlink, and inter-satellite communications. The K- and Ka-bands can be operated with miniaturized antenna system and can provide excellent solutions for high channel capacity required for large variety of end users and high data rate wireless applications [7]. K-band covers the microwave frequencies ranging from 18 to 27 GHz. Recently, K-band is employed for various applications of satellite communications and many astronomical applications including deep space observations. Radars employing the K-band of the frequency are short-range and can achieve target detection and identification with very high

Received 15 September 2022, Accepted 27 October 2022, Scheduled 31 October 2022
* Corresponding author: Khalid Fawzy Ahmed Hussein (fkhalid@eri.sci.eg).
[1] Belbis High Institute of Engineering, Belbis, Egypt. [2] Electronics Research Institute (ERI), Cairo 11843, Egypt. [3] Faculty of Electronic Engineering, Menoufia University, Menoufia, Egypt. [3] Electronics Research Institute (ERI), Cairo 11843, Egypt.

resolution [8]. Ka-band covers the microwave and millimetre-wave frequencies ranging from 27 GHz to 40 GHz. Many applications operating in Ka-band can offer wide spatial coverage by employing antennas with multiple beams high data rate for wireless communications. Also, the Ka-band of the frequency supports many applications including satellite communications [9], high-resolution radars, and military applications.

Recently, printed antennas of compact size, low profile, and mechanical robustness have growing demand due to their ability to comply with the requirements of the various applications of wireless communications especially those requiring light-weight and conformal antenna structures [6]. Over the last few years, planar and printed antenna structures have attracted the attention of the majority of researchers in the field of radar systems, satellite communications, and high data rate wireless applications. In the recent literature, a variety of antennas have been presented and investigated for operation in the K/Ka band. In [2], a dual wideband semi-circular modified T-shape slot shape microstrip patch antenna is proposed for Ku/K band applications. In [10], a dual-band (K- and Ka-bands) antenna printed on a planar multilayered structure is proposed for satellite communications where the uplink operates at 30 GHz, and the downlink operates at 20 GHz. In [11], a patch antenna is proposed to operate in the X-, Ku-, and K-bands of the frequency. A dual-band double-layer printed antenna is proposed for K- and Ka-band applications in [12], where a driven patch is printed on the lower layer whereas the upper layer has non-periodic array.

The present work aims to design a wideband planar antenna printed on a single side of a thin dielectric substrate to cover the band (18–40 GHz). A novel method is proposed for enhancing the bandwidth and efficiency by constructing the monopole patch antenna using multiple merged circular sector patch radiators and feeding the antenna through a coplanar waveguide (CPW) with a wide central strip.

After the introduction section, the present paper has the following organization. Section 2 explains the design of the proposed antenna and presents parametric study to arrive at the optimum design. Section 3 describes the antenna fabrication and measurement of the reflection coefficient at the antenna feeding port and provides a comparison with the simulation results. Section 4 presents the radiation patterns. Section 5 demonstrates the dependence of the gain and radiation efficiency on the frequency. Section 6 provides some comparisons with other wideband antennas presented in recently published work. Finally, Section 7 summarizes the conclusions of the present work.

2. ANTENNA DESIGN

This section is concerned with the detailed description of the proposed design of the multi-leaf-shaped antenna introduced in the present work.

2.1. Geometry of the Proposed Antenna

The geometrical design of the proposed antenna is based on merging multiple wideband radiators into one structure. When the antenna geometry is described by angles rather than lengths this results in a very wide band. Figure 1(a) shows a circular sectorial leaf-shaped patch antenna whose geometry is described by the apex angle Ψ and radius R_P. This is an example of a wideband patch antenna whose geometry is described by one angular dimension and one length dimension. The bandwidth is further increased by feeding this patch antenna through a CPW. Five units of this leaf-shaped patch are sequentially rotated and merged to construct a multi-leaf-shaped patch antenna that is fed through a CPW as shown in Figure 1(b). In the resulting antenna structure, the angle, Φ_R, of sequential rotation adds a new angular dimension to the composite antenna geometry. As shown in Figure 1(b), each one of the five patches is rotated by an angle that is integer multiples Φ_R about the end point of the CPW feeder before being merged into the composite patch antenna that is presented in Figure 1(c). Thus, the final geometry of the five-leaf-shaped patch antenna is described as three dimensions; the two angles, Ψ and Φ_R, and the radius, R_R. This enhances the bandwidth of the proposed monopole patch antenna. The other dimensions are those of the feeding CPW: the feeder length, L_G, central strip width, W_F, slot width, W_G, and length L_G of the strip connecting the CPW feeder to the patch. The composite patch antenna and CPW feed line are printed on a single face of Rogers' RO3003 substrate of $\epsilon_r = 3$,

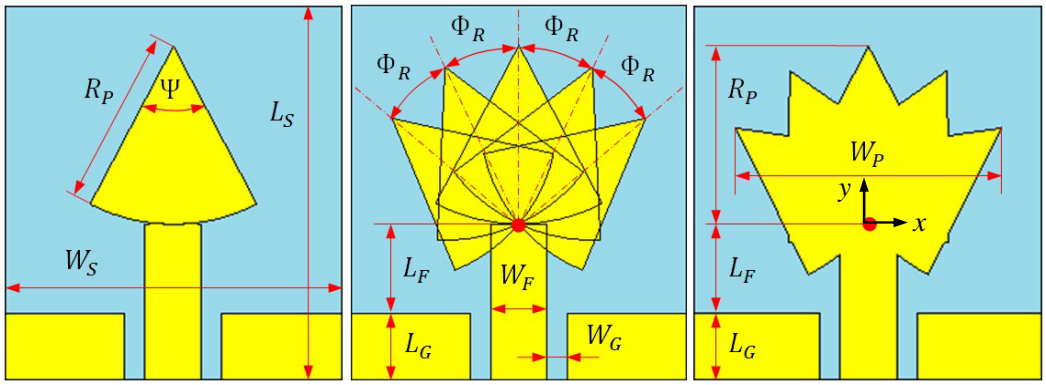

(a) (b) (c)

Figure 1. Construction of the five-leaf-shaped patch antenna. (a) Single leaf-shaped patch antenna fed through CPW. (b) Five leaf-shaped patches with sequential rotations. (c) Geometry of the composite patch antenna proposed in the present work.

thickness $h = 0.13\,\text{mm}$ and loss tangent $\tan\delta = 0.001$. It should be noticed that the width W_P of the composite five-leaf-shaped patch radiator, shown in Figure 1(c), is not an independent dimension as it can be calculated from the radius, R_P, of the single leaf-shaped patch and the angle, Φ_R, as follows.

$$W_P = 2R_P \sin 2\Phi_R \tag{1}$$

The antenna design process has been achieved through extensive parametric study to select the values of the dimensional parameters presented in Figure 1 for the widest impedance matching frequency band and the highest radiation efficiency. The optimal dimensions of the proposed antenna are listed in Tables 1 and 2. These dimensions are obtained through many parametric studies to get the widest bandwidth for impedance matching and the maximum radiation efficiency over the operational bandwidth (18–40 GHz). Section 2.2 presents some examples of the most important parametric studies concerned to enhance the antenna performance.

Table 1. List of dimensions of the five-leaf-shaped patch (the radiator).

Length Dimension	R_P	W_P
Value (mm)	4.4	6.72

Angular Dimension	Ψ	Φ_R
Value	55°	25°

Table 2. List of dimensions of the CPW feeder and the substrate.

Length Dimension	L_F	W_F	L_G	W_G	L_S	W_S
Value (mm)	2.2	1.38	1.65	0.5	9.25	8.2

2.2. Optimization of the Antenna Design through Parametric Study

The dimensional parameters of the antenna design presented in Figure 1 can be optimized to maximize the radiation efficiency and operational bandwidth so as to realize high performance operation over the desired frequency band (18–40 GHz). The parametric studies performed through electromagnetic simulation can achieve these goals by finding the best values of the most important dimensions that affect the antenna performance including the leaf apex angle Ψ, radius R_P, angle of rotation Φ_R, and CPW feeder length L_G.

The effect of changing the radius R_P on the behavior of $|S_{11}|$ with the frequency is depicted in Figure 2. It is clear that increasing R_P results in shifting the lower frequency of the impedance matching band to the left. Also, increasing R_P leads to decreasing the minimum value of $|S_{11}|$ and results in shifting the corresponding frequency to the left. The widest bandwidth for impedance matching ($|S_{11}| < -10\,\text{dB}$) is obtained when $R_P = 4.4\,\text{cm}$.

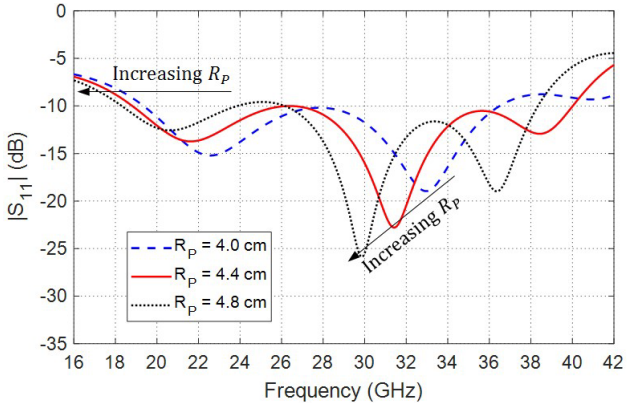

Figure 2. Influence of changing the radius R_P on the frequency response of $|S_{11}|$ of the proposed antenna.

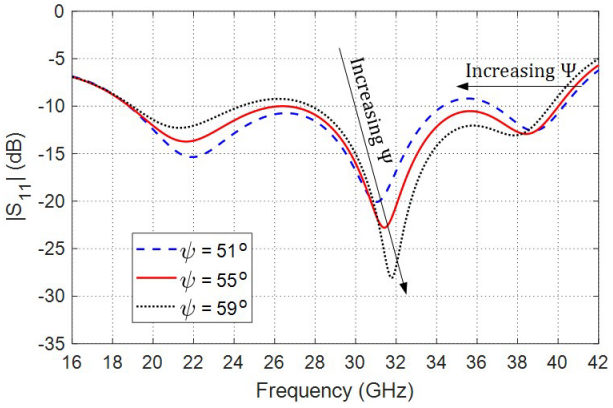

Figure 3. Influence of changing the apex angle Ψ on the frequency response of $|S_{11}|$ of the proposed antenna.

Changing the leaf apex angle, Ψ, affects the frequency response of $|S_{11}|$ as shown in Figure 3. Increasing the angle Ψ leads to decreasing the higher frequency of the band of impedance matching. Also, the minimum of $|S_{11}|$ is decreased, and the corresponding frequency is slightly increased with increasing Ψ. As shown in Figure 3, the widest frequency band of impedance matching is obtained when $\Psi = 55°$.

The frequency response of $|S_{11}|$ is affected by changing the angle of rotation Φ_R as shown in Figure 4. Increasing the angle Φ_R leads to increasing the lower frequency of the band over which $|S_{11}| < -10\,\text{dB}$. Also, the minimum of $|S_{11}|$ is decreased, and the corresponding frequency is decreased when Φ_R is increased. As shown in Figure 4, the widest frequency band of impedance matching is obtained when $\Phi_R = 25°$.

Changing the length, L_G, of the CPW feeder affects the frequency response of $|S_{11}|$ as depicted in Figure 5. Increasing the length L_G leads to decreasing the lower as well as higher frequencies of the

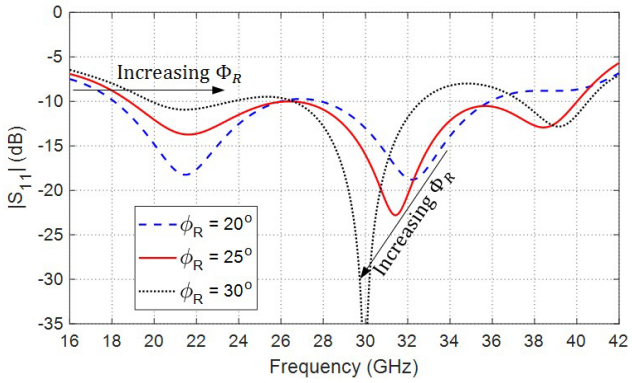

Figure 4. Influence of changing the angle of rotation Φ_R on the frequency response of $|S_{11}|$ of the proposed antenna.

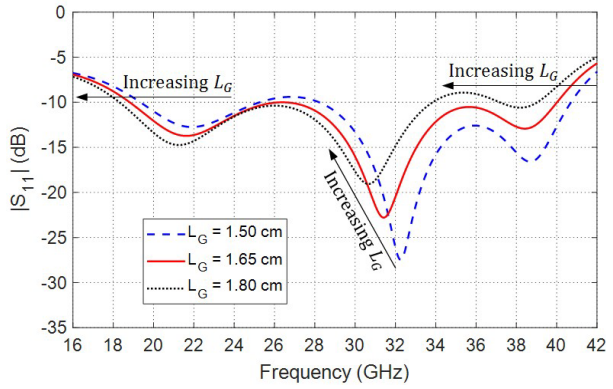

Figure 5. Influence of changing the feeder length, L_G, on the frequency response of $|S_{11}|$ of the proposed antenna.

band of impedance matching ($|S_{11}| < -10\,\text{dB}$). Also, it is noticed that the minimum of $|S_{11}|$ is increased with increasing L_G, and the corresponding frequency is decreased. It is clear that setting $L_G = 1.65\,\text{cm}$ gives the widest frequency band over which the antenna impedance is matched.

The parametric studies demonstrated in the present sections are examples of the extensive studies that are required to obtain the best dimensions of the antenna design presented in Figure 1(c). The objectives of such studies are to get the widest impedance matching bandwidth and to enhance radiation efficiency. Also, it is required to get the impedance matching frequency extending from 18 GHz to 40 GHz as exactly as possible. The complete parametric studies lead to the optimal design parameters listed in Tables 1 and 2.

3. FABRICATION OF THE ANTENNA AND MEASUREMENT OF THE RETURN LOSS

For practical assessment of the proposed antenna performance, a prototype is fabricated for experimental measurement. It should be noted that the dimensions listed in Tables 1 and 2 are used for fabrication. The fabricated prototype of the five-leaf-patch antenna is presented in Figure 6(a). A standard coaxial launcher is attached to the fabricated prototype. As shown in this figure, the antenna and feeding CPW are printed on one face of the Rogers' substrate whereas the other face is left blank. The overall size of the antenna with the attached launcher is compared to the size of a coin of one-inch diameter. The measurement of S_{11} is achieved by means of the vector network analyzer (VNA) model Rhode & Schwarz-ZVA67 as shown in Figure 6(b).

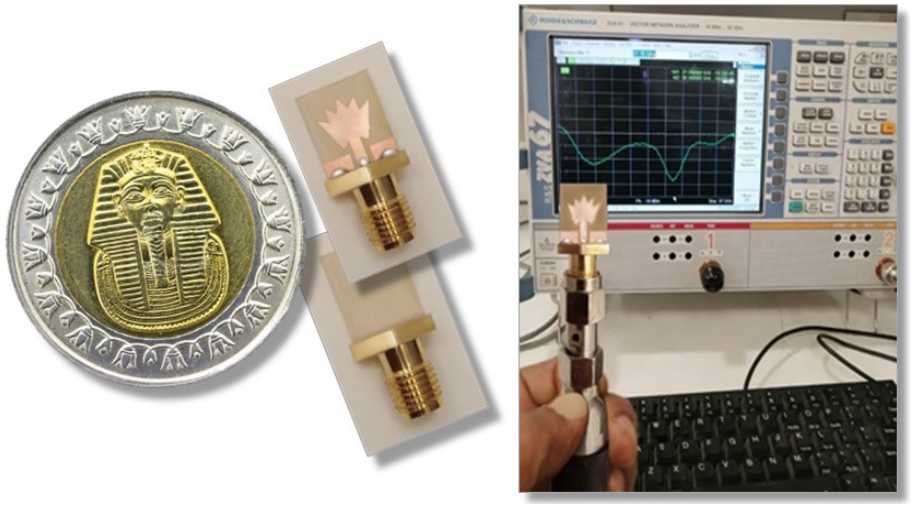

(a) (b)

Figure 6. (a) Top and bottom views of the fabricated prototype of the proposed antenna. (b) The antenna is connected to the VNA for measuring S_{11}.

The measured frequency response of $|S_{11}|$ is presented in Figure 7 in comparison to the results of simulation. It is clear that the results obtained through measurement show good agreement with the results of simulation. Both the experimental and simulatied results show that $|S_{11}| < -10\,\text{dB}$ over the band of frequencies 18–40 GHz.

4. EVALUATION OF THE FAR FIELD PATTERNS

In this section, the far field patterns are obtained by the CST® simulator over the entire frequency band suggested for the antenna operation (18–40 GHz). The far field patterns at 28 GHz are obtained by both simulation and experimental measurement for the sake of validation through comparison.

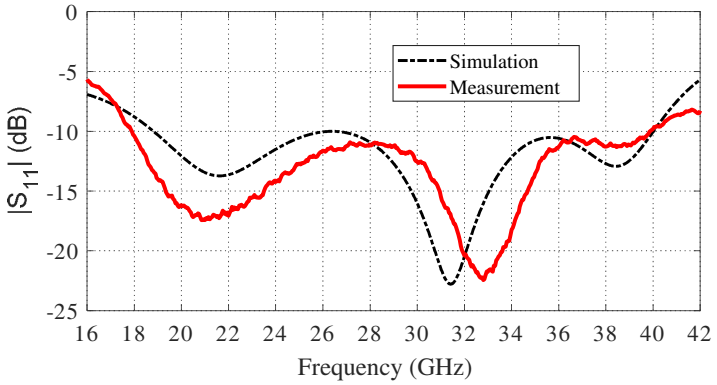

Figure 7. Experimental and simulation results for the frequency response of the reflection coefficient magnitude, $|S_{11}|$, over the frequency band (16–42 GHz).

4.1. Evaluation of the Radiation Patterns over the Frequency Band of Operation

The far field patterns obtained by simulation in the azimuth and elevation planes, $\phi = 0°$ and $\theta = 90°$, respectively, are presented in Figure 8. It is shown that the far field patterns are omnidirectional except for those evaluated at the center frequencies of the impedance matching band. At the lower and higher frequencies of the operational band (18 and 40 GHz), the far field patterns have nearly circular symmetry in the azimuth plane, $\phi = 0°$. Near the center frequencies of the operational band, the far field is reduced in the directions ($\theta = 90°$). It is shown that the far field patterns have 8-figure in the elevation plane, $\theta = 90°$, with the nulls of the 8-figure in the directions $\phi = 90°$ and $\phi = 270°$. Some deformations of the 8-figure resulting from extra nulls encountered at the higher frequencies are noticed in Figure 8(b).

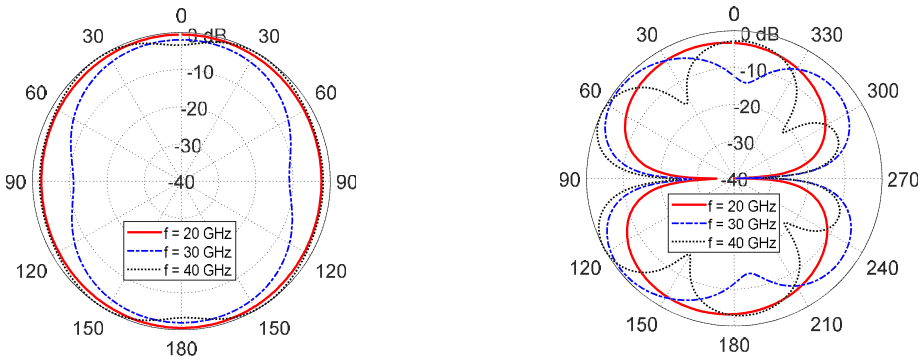

Figure 8. Far field patterns of the five-leaf-shaped printed antenna over the frequency band of operation in two orthogonal planes, (a) azimuth plane $\phi = 0°$, and (b) elevation plane $\theta = 90°$.

4.2. Simulation and Experimental Evaluation of the Radiation Patterns

To validate the radiation patterns obtained by simulation for the proposed antenna, they are compared with the experimental measurements. Figure 9 presents comparisons between the far field patterns as measured at 28 GHz in the azimuth and elevation planes $\phi = 0°$ and $\theta = 90°$, respectively, compared to the patterns obtained by the CST® simulator. The experimental and simulated results show good agreement with each other.

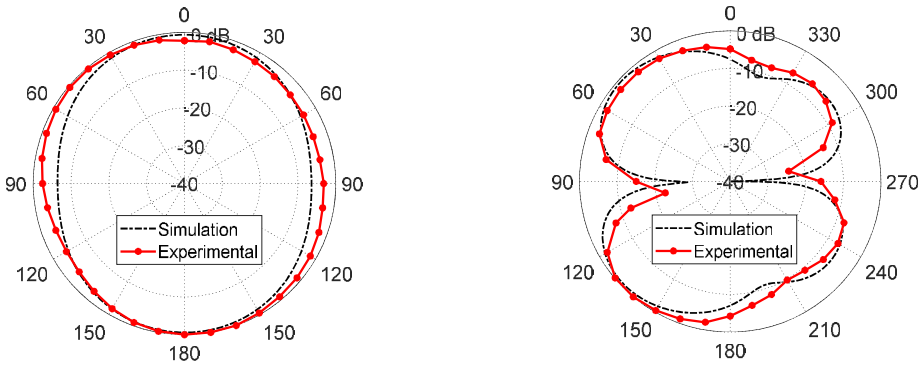

(a) (b)

Figure 9. The measured radiation patterns of the proposed antenna at 28 GHz compared to those obtained by simulation in two orthogonal planes, (a) azimuth plane $\phi = 0°$ and (b) elevation plane $\theta = 90°$.

5. FREQUENCY RESPONSE OF THE GAIN AND RADIATION EFFICIENCY

The variations of the maximum gain produced by the proposed antenna and the associated radiation efficiency are evaluated over the frequency band (18–40 GH). Figure 10 shows the frequency response of the maximum gain over the frequency band of operation. It is shown that the experimental and simulated results come in good agreement, and both of them show that the maximum gain ranges from 3 to 4.6 dBi over the entire frequency band with a peak value about 4.6 dBi at 34 GHz.

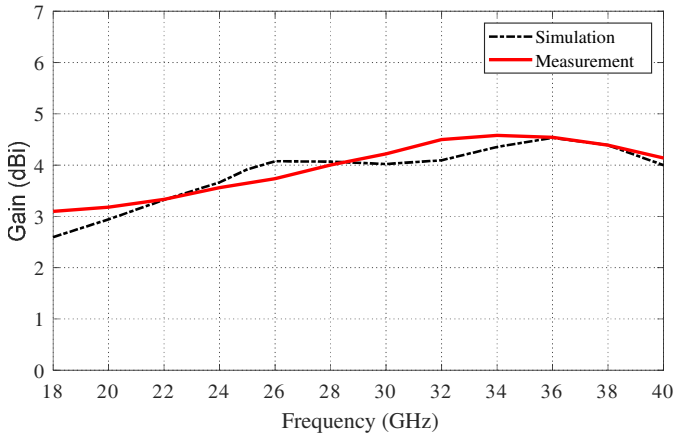

Figure 10. Frequency response of the maximum gain of the proposed antenna over the entire frequency band.

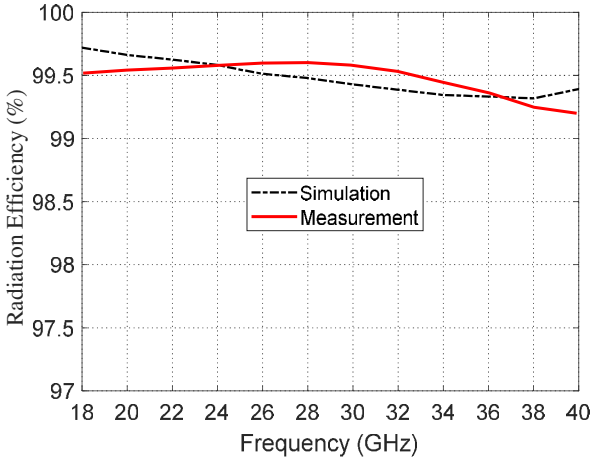

Figure 11. Frequency response of the radiation efficiency of the proposed antenna over the entire frequency band.

The frequency response of the radiation efficiency over the entire frequency band is depicted in Figure 11. As shown in the figure, the antenna has perfect radiation efficiency over the entire frequency band. The average radiation efficiency over the entire band is about 99.5%. Such high performance regarding the radiation efficiency of the proposed wideband antenna can be attributed to (i) the small antenna size, (ii) the thin dielectric substrate, (iii) the low tangent loss of the Rogers' RO3003 substrate material, (iv) printing the antenna and the feeding line on one face of the substrate, and (v) wide central strip of the CPW feeder.

6. COMPARATIVE ASSESSMENT OF THE ANTENNA PERFORMANCE

The size and the most important performance measures of the proposed monopole patch antenna are compared to those available in some recently published works. The results of comparison are listed in Table 3. The comparative performance involves the impedance matching bandwidth, maximum gain, and radiation efficiency.

Table 3. Comparative evaluation of the proposed antenna performance with recently published antenna designs.

Work	Dimensions (mm × mm)	Frequency Bands (GHz)	Bandwidth (GHz)	Gain (dBi)	Radiation Efficiency (%)
[2]	30 × 15	16.6–18.7 22.6–23.4	2.9	6.5	68
[10]	4.17 × 5.23	18–21.5 28.5–32.5	7.5	NA	NA
[11]	8 × 16	7.6–10.4 14.5–18 19.2–20	7.1	7	80
[12]	8 × 8	15.7–16.2 29.9–31.1	1.7	7.2	NA
[13]	21 × 15	6–21	15	4.5	82
[Present]	9.25 × 8.2	18–40	22	4.5	99.2

7. CONCLUSION

A novel design of miniature multi-leaf-shaped monopole patch antenna has been introduced for operation in the K and Ka frequency bands. It has been shown through simulation and experimental work that the proposed antenna has a frequency band extending from 18 to 40 GHz. The proposed antenna has been fabricated on a Rogers' RO3003 dielectric substrate of 0.25 mm thickness. To enhance the frequency bandwidth of this antenna, it has been constructed as five circular sectors placed with sequential rotations and merged to form the monopole patch antenna. The monopole patch is fed through a CPW structure, which enables the overall antenna structure with the feeding line to be printed on only one side of the dielectric substrate leaving the other side blank. A prototype of the antenna has been fabricated for experimental assessment. It has been shown that the antenna has 2.2 : 1 ratio bandwidth, 76% percentage bandwidth, and 278 bandwidth-dimension ratio. The radiation efficiency is maintained above 99% over the entire bandwidth (18–40 GHz).

REFERENCES

1. Eichler, J., P. Hazdra, M. Capek, T. Korinek, and P. Hamouz, "Design of a dual-band orthogonally polarized L-probe-fed fractal patch antenna using modal methods," *IEEE Antennas Wireless Propag. Lett.*, Vol. 10, 1389–1392, 2011.
2. Singh, V., B. Mishra, and R. Singh, "Dual-wideband semi-circular patch antenna for Ku/K band applications," *Microwave and Optical Technology Letters*, Vol. 61, No. 2, 323–329, 2019.
3. Singh, V., B. Mishra, P. N. Tripathi, and R. Singh, "A compact quad-band microstrip antenna for S and C-band applications," *Microwave and Optical Technology Letters*, Vol. 58, No. 6, 1365–1369, 2016.
4. Mishra, B., V. Singh, and R. Singh, "Dual and wide-band slot loaded stacked microstrip patch antenna for WLAN/WiMAX applications," *Microsyst Technol.*, Vol. 23, No. 8, 3467–3475, 2017.

5. Chandel, R. and A. K. Gautam, "Compact MIMO/diversity slot antenna for UWB applications with band-notched characteristic," *Electron Lett.*, Vol. 52, No. 5, 336–338, 2016.
6. Samsuzzaman, M., M. T. Islam, and J. S. Mandeep, "Triple band X shape microstrip patch antenna for Ku/K band applications," *Modern Applied Science*, Vol. 7, No. 8, 70, 2013.
7. Feltrin, E. and E. Weller, "New frontiers for the mobile satellite interactive services," *5th Advanced Satellite Multimedia Systems Conference and the 11th Signal Processing For Space Communications Workshop*, 155–161, 2010.
8. Rafique, U. and S. A. Ali, "Ultra-wideband patch antenna for K-band applications," *TELKOMNIKA Indonesian Journal of Electrical Engineering*, Vol. 12, No. 12, 8252–8256, 2014.
9. https://resources.system-analysis.cadence.com/blog/msa2022-the-applications-and-advantages-of-ka-band-frequency.
10. Chaloun, T., C. Hillebrand, C. Waldschmidt, and W. Menzel, "Active transmitarray submodule for K/Ka band satcom applications," *2015 German Microwave Conference*, 198–201, IEEE, 2015.
11. Mishra, B., "An ultra compact triple band antenna for X/Ku/K band applications," *Microwave and Optical Technology Letters*, Vol. 61, No. 7, 1857–1862, 2019.
12. Kandwal, A., "Compact dual band antenna design for Ku/Ka band applications," *Advanced Electromagnetics*, Vol. 6, No. 4, 1–5, 2017.
13. Saini, A. S., A. Sharma, P. Srivastava, and K. Anjali, "Design of wideband microstrip antenna for X, Ku and K-band applications," *2021 International Conference on Advance Computing and Innovative Technologies in Engineering (ICACITE)*, 723–725, IEEE, 2021.